UNIVERSITY *of* York

This is a repository copy of *Dehydropolymerization of H3B·NMeH2 Using a [Rh(DPEphos)]+ Catalyst:The Promoting Effect of NMeH2*.

White Rose Research Online URL for this paper:
https://eprints.whiterose.ac.uk/155078/

Version: Published Version

Article:

eprints@whiterose.ac.uk
https://eprints.whiterose.ac.uk/

Catalysis

Dehydropolymerization of $H_3B \cdot NMeH_2$ Using a [Rh(DPEphos)]$^+$ Catalyst: The Promoting Effect of $NMeH_2$

Gemma M. Adams,[†] David E. Ryan,[†] Nicholas A. Beattie,[‡,||] Alasdair I. McKay,[†] Guy C. Lloyd-Jones,[§] and Andrew S. Weller*,[†]

[†]Chemistry Research Laboratories, Mansfield Road, University of Oxford, Oxford OX1 3TA, United Kingdom
[‡]Institute of Chemical Sciences, Heriot Watt University, Edinburgh EH14 4AS, United Kingdom
[§]School of Chemistry, University of Edinburgh, Edinburgh EH9 3FJ, United Kingdom

Ⓢ Supporting Information

ABSTRACT: $[Rh(\kappa^2\text{-}PP\text{-}DPEphos)\{\eta^2\eta^2\text{-}H_2B(NMe_3)\text{-}(CH_2)_2{}^tBu\}][BAr^F_4]$ acts as an effective precatalyst for the dehydropolymerization of $H_3B \cdot NMeH_2$ to form N-methyl-polyaminoborane $(H_2BNMeH)_n$. Control of polymer molecular weight is achieved by variation of precatalyst loading (0.1−1 mol %, an inverse relationship) and use of the chain-modifying agent H_2: with M_n ranging between 5 500 and 34 900 g/mol and $Đ$ between 1.5 and 1.8. H_2 evolution studies (1,2-$F_2C_6H_4$ solvent) reveal an induction period that gets longer with higher precatalyst loading and complex kinetics

with a noninteger order in $[Rh]_{TOTAL}$. Speciation studies at 10 mol % indicate the initial formation of the amino−borane bridged dimer, $[Rh_2(\kappa^2\text{-}PP\text{-}DPEphos)_2(\mu\text{-}H)(\mu\text{-}H_2BN=HMe)][BAr^F_4]$, followed by the crystallographically characterized amidodiboryl complex $[Rh_2(cis\text{-}\kappa^2\text{-}PP\text{-}DPEphos)_2(\sigma,\mu\text{-}(H_2B)_2NHMe)][BAr^F_4]$. Adding ~2 equiv of $NMeH_2$ in tetrahydrofuran (THF) solution to the precatalyst removes this induction period, pseudo-first-order kinetics are observed, a half-order relationship to $[Rh]_{TOTAL}$ is revealed with regard to dehydrogenation, and polymer molecular weights are increased (e.g., M_n = 40 000 g/mol). Speciation studies suggest that $NMeH_2$ acts to form the precatalysts $[Rh(\kappa^2\text{-}DPEphos)(NMeH_2)_2][BAr^F_4]$ and $[Rh(\kappa^2\text{-}DPEphos)(H)_2(NMeH_2)_2][BAr^F_4]$, which were independently synthesized and shown to follow very similar dehydrogenation kinetics, and produce polymers of molecular weight comparable with $[Rh(\kappa^2\text{-}PP\text{-}DPEphos)\{\eta^2\text{-}H_2B(NMe_3)\text{-}(CH_2)_2{}^tBu\}][BAr^F_4]$, which has been doped with amine. This promoting effect of added amine in situ is shown to be general in other cationic Rh-based systems, and possible mechanistic scenarios are discussed.

KEYWORDS: dehydropolymerization, rhodium, amine−borane, mechanism, DPEphos
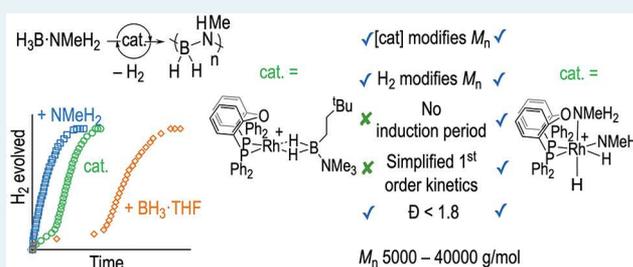
1. INTRODUCTION

Polyaminoboranes,[1−4] exemplified by N-methylpolyaminobor-ane $(H_2BNMeH)_n$, have alternating main-chain B−N units and are of interest as precursors to BN-based ceramics or as new unexplored materials that are isosteres of polyolefins. Since the original report of the synthesis of $(H_2BNMeH)_n$ by the dehydropolymerization of $H_3B \cdot NMeH_2$ using an Ir(POCOP)-H_2 catalyst (POCOP = $\kappa^3\text{-}C_6H_3\text{-}2,6\text{-}(OP^tBu_2)_2$),[4−6] there has been significant progress in developing catalytic method-ologies,[7−13] as well as noncatalyzed routes.[14] The accepted overarching catalytic mechanism operates via initial dehydro-genation of $H_3B \cdot NMeH_2$ to form a transient free, or metal-bound amino−borane, which then undergoes a head-to-tail BN coupling (Scheme 1). A number of different propagation scenarios have been proposed for this latter step that show elements of chain-growth,[4,10] step-growth,[15] or hybrid mechanisms.[16] Particularly interesting would be systems that demonstrate the potential for control[17] over the polymer-ization process, holistically defined by degree of polymerization (as measured by M_n), dispersity ($Đ$), initiation/termination

Scheme 1. Dehydropolymerization of Amine−Boranes
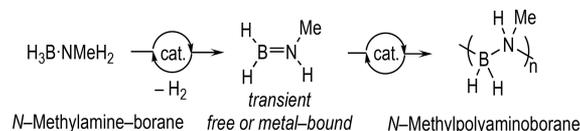
events, and catalyst lifetime (i.e., TON). While aspects of these performance criteria have been noted,[7−10,15] there is no general approach to their optimization.
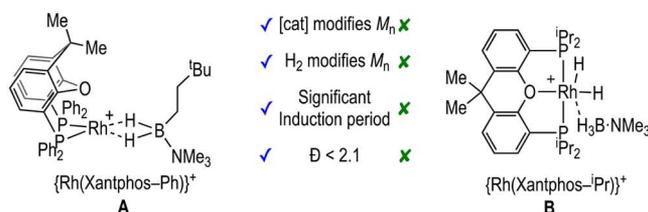
We have reported cationic dehydropolymerization precata-lysts based upon {Rh(Xantphos-R)}$^+$ motifs,[18,19] in which the identity of the PR_2 group is changed (Scheme 2).[9,10,20] When R = Ph (**A**), medium[2] molecular weight polymer is formed (M_n = 22 700 g/mol, $Đ$ = 2.1), a higher catalyst loading promotes lower M_n, and H_2 acts to modify the polymer chain length (M_n

Scheme 2. Comparison of Previously Reported Rh–Xantphos-Based Catalysts and Their Performance in Dehydropolymerization of $H_3B \cdot NMeH_2$; $[BAr^F_4]^-$ Anions Not Shown


Scheme 3. Synthesis of the $\{Rh(DPEphos)\}^+$ Precatalyst 2a

= 2 800 g/mol, Đ = 1.8). Although detailed kinetics for $H_3B \cdot NMeH_2$ dehydropolymerization were not reported, these observations were interpreted as signaling a coordination/insertion/chain-growth mechanism in concert with more extensive studies on $H_3B \cdot NMe_2H$.[9] There is also a significant induction period observed (~10 min). In contrast, when R = ^iPr (**B**), H_2 and catalyst loading do not significantly change M_n (9 500 g/mol, Đ ≈ 2.8), there is a negligible induction period, and a dual role[11,12] for the organometallic species was proposed in which dehydrogenation/propagation occurs from different metal centers. This mechanistic switch may be influenced by the preferred ligand-coordination modes:[21] Xantphos-Ph is a hemilabile ligand preferring to coordinate cis-κ^2-PP and mer-κ^3-POP, while Xantphos-^iPr prefers mer-κ^3-POP (Figure S1 compares coordination modes for crystallographically characterized Xantphos-R complexes).

We now report a detailed and systematic study on the dehydropolymerization of $H_3B \cdot NMeH_2$ using a different Rh-POP-based system: $\{Rh(DPEphos)\}^+$ [DPEphos = bis(2-(diphenylphosphino)phenyl)ether]. Using this ligand, which favors cis-κ^2-PP coordination (Figure S1), significant control over M_n by both catalyst loading and H_2 is achieved, with M_n ranging from 5 500 to 40 000 g/mol and Đ = 1.5–1.8. These studies also reveal the formation of dimeric species, and the key role of added amine, $NMeH_2$, in both promoting catalysis and increasing M_n/lowering Đ of the isolated polymer. Finally, combining these observations, the synthesis and evaluation in catalysis of a simple $[Rh(\kappa^2$-PP-DPEphos)$(NMeH_2)_2]^+$ precatalyst is reported. This positive influence of added amine is also shown to be general for other previously reported cationic Rh-based systems. The role of added amine has been recently noted with regard to increasing catalyst lifetime of Ru-based catalysts for the dehydropolymerization of $H_3B \cdot NH_3$ by trapping BH_3 formed from B–N bond cleavage,[8] although the influence of amine on the characteristics of the polymer produced were not commented upon.

2. RESULTS AND DISCUSSION

2.1. Precatalyst Synthesis. Precatalyst **2a**, $[Rh(\kappa^2$-P,P-DPEphos)$\{\eta^2\eta^2$-$H_2B(NMe_3)(CH_2)_2{}^tBu\}][BAr^F_4]$ (Ar^F = 3,5-$(CF_3)_2C_6H_3$), is synthesized from hydroboration of ^{t}butylethene (TBE) by $H_3B \cdot NMe_3$ using the NBD precursor **1a** (NBD = norbornadiene), preactivated by H_2 (Scheme 3). Spectroscopic data for purple **2a** are similar to the previously reported Xantphos-Ph derivative, **A**.[22] In particular, a single environment is observed in the $^{31}P\{^1H\}$ NMR spectrum [δ 40.0 ppm, J(RhP) = 180 Hz], the 3-center, 2-electron Rh···H–B groups are observed at δ −5.55 ppm (2 H) in the ^1H NMR spectrum, while the ^{11}B NMR spectrum shows a characteristically[23] downfield-shifted resonance [δ 33.3 ppm], indicating a
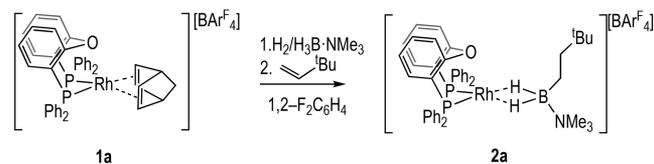
bidentate binding mode of the borane. The amine–borane in **2a** is easily displaced, and the $[Rh(Xantphos-Ph)]^+$ analogue (**A**) has been shown to be active for $H_3B \cdot NMeH_2$ dehydropolymerization,[9] TBE hydroboration using $H_3B \cdot NMe_3$,[24] and B–B homocoupling.[22]

2.2. Dehydropolymerization of $H_3B \cdot NMeH_2$: Variation of Conditions. Precatalyst **2a** is an effective for dehydropolymerization, and full conversions of $H_3B \cdot NMeH_2$ are obtained even at low loadings under a slow stream of Ar to remove H_2 (e.g., 0.223 M $H_3B \cdot NMeH_2$, [**2a**] = 0.1 mol %, TON = 1000, 6 h). Variation of precatalyst loadings between 0.2 and 1 mol % reveals an inverse relationship between M_n of the isolated polymer and catalyst loading (Table 1, entries 1–3, and Figure 1A). The resulting ^{11}B NMR spectra of the reaction mixtures and isolated polymer show the characteristic[2,12] broad signal at δ −6 ppm for $(H_2BNMeH)_n$ and only trace $(HBNMe)_3$ (Figure S18). The $^{13}C\{^1H\}$ NMR spectra (H_8-THF) show a relatively sharp peak at δ 35.5 ppm (NMe). In contrast, at 0.1 mol % catalyst loading, M_n does not increase compared to 0.2 mol %, and there is significant 1,2-$F_2C_6H_4$ insoluble polymer that is tetrahydrofuran (THF)-soluble. NMR spectroscopic analysis of this material (Figure S19) showed additional signals at δ(^{11}B) ~1 ppm and δ($^{13}C\{^1H\}$) ~35.7 ppm (br, NMe) that may signal tertiary or quaternary main-chain centers, suggesting cross-linking/chain branching.[10,11,19,25] While we currently have no explanation for this change in polymer characteristics, at these very low loadings trace impurities (or products of B–N bond cleavage, vide infra) may have a disproportionate effect on the polymerization process, leading to a different product being formed. When dehydropolymerization was conducted under H_2 measurement conditions (eudiometer, H_2 established in the head space), or in a closed system that allows for H_2 buildup, H_2 likely acts as a chain-transfer/termination agent and significantly shorter polymer is isolated, for which a significantly larger signal at δ(^{11}B) ~−18 ppm is observed, which could be assigned to BH_3 end groups[15] (Figure 1B; Figure S20 shows a representative ^{11}B NMR spectrum). Similar Đ are retained compared with the open system, as is the inverse relationship between M_n and catalyst loading (Table 1, entries 5–8). Interestingly, there is now a significant difference in M_n between 0.1 and 0.2 mol %, suggesting that H_2 modifies the influence of the very low catalyst loading. A conversion versus M_n study (0.2 mol %, open system, Figure 1C) indicates that a chain-growth mechanism is operating, because at low (10%) conversions long polymer chains are observed (M_n = 24 800 g/mol, Đ = 1.2) and $H_3B \cdot NMeH_2$ monomer dominates (Figure S21).

We have previously, but briefly, reported similar control of molecular weight by catalyst loading and H_2 for catalyst **A** and suggested a coordination/dehydrogenation/insertion/chain-growth mechanism for the dehydropolymerization, in which the same metal center both dehydrogenates an amine–borane and promotes propagation.[9] This more comprehensive data with **2a** supports a similar mechanism in the $\{Rh(DPEphos)\}^+$ system. That H_2 acts to modify the polymer chain may arise

Table 1. GPC Characterization Data for Isolated Polyaminoborane[a]

entry	catalyst	$[\mathrm{Rh}]_{\mathrm{TOT}}$, mol %	conditions	M_n, g/mol	Đ
1	2a	1	open (Ar flow)	6400	1.8
2	2a	0.4	open (Ar flow)	29500	1.8
3	2a	0.2	open (Ar flow)	34900	1.5
4	2a	0.1	open (Ar flow)	34600	1.7
5	2a	0.1	H_2 measurement	29400	1.6
6	2a	0.2	H_2 measurement	14500	1.7
7	2a	0.4	H_2 measurement	10100	1.8
8	2a	1	H_2 measurement	5500	1.8
9	3a	0.4	H_2 measurement	14800	1.6
10	4b	0.4	H_2 measurement	15900	1.8
11	2a	0.4	H_2 measurement/1 equiv of $H_3B\cdot THF$/50 μL of THF	6600	1.9
12	2a	0.4	H_2 measurement/10 equiv of $[H_2B(NMeH_2)_2][BAr^F_4]$	2800	2.3
13	2a	0.4	H_2 measurement/50 μL of THF	11000	1.6
14	2a	0.4	H_2 measurement/~2 equiv of $NMeH_2$ in 50 μL of THF	27400	1.6
15	2a	0.4	open/~2 equiv of $NMeH_2$ in 50 μL of THF	32100	1.6
16	5/6	0.2	H_2 measurement	38900	1.6
17	5/6	0.4	H_2 measurement	33200	1.6
18	5/6	1	H_2 measurement	20600	1.5
19	6	0.8	H_2 measurement	22500	1.5
20	2a	0.2	H_2 measurement/~2 equiv of $NMeH_2$ in 50 μL of THF	34800	1.5
21	A[9]	0.2	H_2 measurement	40500	1.7
22	A[9]	0.2	H_2 measurement/~2 equiv of $NMeH_2$ in 50 μL of THF	61900	1.6
23	C[16]	0.2	H_2 measurement	63100	1.7
24	C[16]	0.2	H_2 measurement/~2 equiv of $NMeH_2$ in 50 μL of THF	78900	1.6

[a]All at 298 K, 0.223 M $H_3B\cdot NMeH_2$, 1,2-$F_2C_6H_4$ solvent. GPC data quoted relative to polystyrene standards (calibrated between 500 and 480 000 g/mol), triple column, RI detection, THF with 0.1 w/w% [NBu₄]Br, 35 °C, sample concentration = 2 mg/cm³. Open conditions: periodic sampling by ¹¹B NMR spectroscopy determined end point (e.g., 6 h for entry 4). Under H_2 measurement conditions, the reaction was stopped when there was no significant change in H_2 evolved.

from chain-termination/transfer by hydrogenolysis of a Rh–BH₂(polymeryl) or Rh–NMeH(polymeryl) bond. The use of H_2 as a chain-termination agent in olefin polymerization is well-established, operating through sigma-bond metathesis of [M]-CH₂-polymeryl with H_2 to form a metal hydride and free polymer.[26] The inverse relationship between M_n and catalyst loading suggests dehydropolymerization at a single metal center, as lower catalyst loadings lead to less propagating sites for the concomitantly formed H₂B=NMeH. Interestingly, this relationship between M_n and initiating sites is also reminiscent of a classical radical polymerization mechanism where the net order in initiator is negative,[27] as has been recently noted.[3]

2.3. Speciation Experiments: The Formation of Dimeric Rh₂ Species. With the polymer growth kinetics in hand, we turned to identifying the species that formed during catalysis using NMR spectroscopy. The low catalyst loadings used for polymerization (0.1−1 mol %) meant that these speciation studies were performed instead at 10 mol % 2a to obtain good signal/noise (sealed NMR tube, 1,2-$F_2C_6H_4$). Under these in situ conditions, ¹¹B NMR spectroscopy showed the formation of a mixture of (H₂BNMeH)ₙ, (HBNMe)₃, and (H₂B)₂(μ-H)(NMeH) [td, δ −22.3 ppm[28]], with the latter potentially signaling free BH₃ by loss of amine. ³¹P{¹H} NMR spectroscopy under these conditions showed the initial formation, after 5 min, of two new dimeric complexes: a bridging hydrido-aminoborane 3a, [Rh₂(DPEphos)₂(μ-H)(μ-H₂B=NHMe)][BAr^F_4], and an amidodiboryl 4a, [Rh₂(κ²-P,P-DPEphos)₂(σ,μ-(H₂B)₂NHMe)][BAr^F_4] (Figure 2A). After 2 h 4a is dominant (80%), but the mixture slowly returns to favoring 3a after 5 h (Figure S22). Complex 3a can be prepared as the only organometallic species by addition of H_2/2 equiv of $H_3B\cdot NMeH_2$ to 1a. Boronium $[BH_2(NMeH_2)_2]^+$ [δ −7.1 ppm, J(BH) = 110 Hz, cf. authentic sample δ −7.4 ppm, J(BH) = 117 Hz, 1,2-$F_2C_6H_4$[10]] is also observed under these conditions,[29] in line with the reported mechanism for the formation of analogous complexes with $[Rh_2(R_2P-(CH_2)_nPR_2)_2(\mu\text{-}H)(\mu\text{-}H_2B=NR'_2)]^+$ motifs.[30,31] Here, attack of free amine (from B–N bond cleavage[32]) at a precursor σ-amine−borane complex generates a neutral dimeric Rh−hydride and $[BH_2(NMeH_2)_2]^+$, for which subsequent proton transfer and $NMeH_2$ loss result in the bridging amino−borane motif. NMR and ESI−MS data for 3a are fully consistent with its formulation (Supporting Materials) and are very closely related to previously reported $[Rh_2(^iPr_2P(CH_2)_3P^iPr_2)_2(\mu\text{-}H)(\mu\text{-}H_2B=NH_2)][BAr^F_4]$.[30] Attempts to characterize these products using single-crystal X-ray diffraction were frustrated by the formation of oily materials. The identity of 4 was only revealed using the $[Al(OC(CF_3)_3)_4]^-$ anion,[33] by a single-crystal study of 4b, $[Rh_2(\kappa^2\text{-}P,P\text{-}DPEphos)_2(\sigma,\mu\text{-}(H_2B)_2NHMe)][Al(OC(CF_3)_3)_4]$, which comes from a slow (days) recrystallization of 3b, formed in situ from [Rh(κ²-P,P-
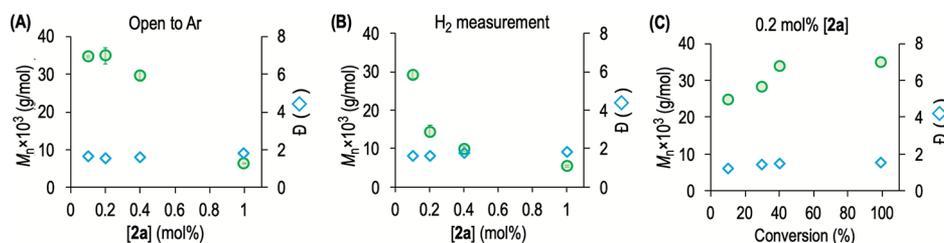
Figure 1. GPC data (relative to polystyrene standards, RI detection, THF with 0.1 w/w% [NBu₄]Br, 35 °C) for (H₂BNMeH)ₙ isolated from $H_3B\cdot NMeH_2$ dehydropolymerization (0.223 M, 1,2-$F_2C_6H_4$, 20 °C) using catalyst 2a. (A) Variation of [2a] under Ar purge; (B) variation of [2a] under H_2 measurement conditions (eudiometer); (C) conversion versus M_n/Đ plot, open conditions, where each individual data point is a PPh₃-quenched experiment after an appropriate time.

Figure 2. (A) Addition of H$_3$B·NMeH$_2$ to **2a** (10 mol %) to form **3a** and **4a**, 1,2-F$_2$C$_6$H$_4$ solvent. (B) Synthesis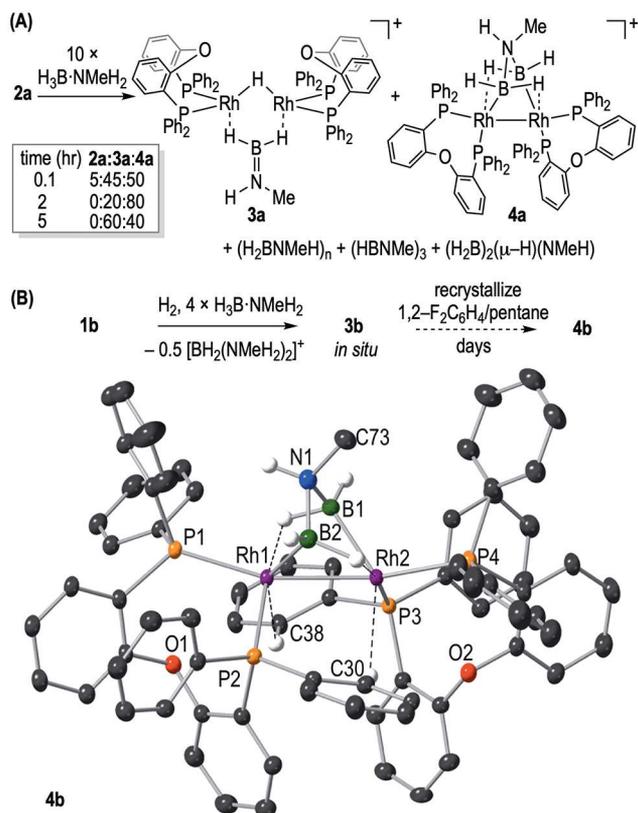 and solid-state structure of the cationic portion of **4**. Selected bond lengths (Å) and angles (deg): Rh1−Rh2 2.6421(4); Rh1−B1 2.326(5), Rh1−B2 2.096(6); Rh2−B1 2.107(5), Rh1−B2, 2.328(5); Rh1−C38 2.997(5), B1−N1, 1.59(1), B2−N1 1.56(1); P1−Rh1−Rh2 162.59(3), P2−Rh1−Rh2, 95.31(3).

D P E p h o s) (N B D)] [A l (O C (C F$_3$)$_3$)$_4$] **1 b** / H$_3$B· NMeH$_2$ activated with H$_2$ (Figure 2B). **4b** is not isolated pure, formed alongside **3b** (∼5% by ^{31}P{^{1}H} NMR spectroscopy) and (H$_2$BNMeH)$_n$. The NMR data for **4b**, aside from the signals due to the anion, are the same as for **4a**, as are the ESI−MS data.

The structure of the cation in **4b** has a Rh$_2$ core [Rh−Rh 2.6421(4) Å] with a bridging amido−bisboryl ligand that has two α-BH···Rh agostic interactions with the proximal Rh centers [e.g., Rh2−B1 2.107(5), Rh1···B1 2.326(5) Å]. Such a description results in formally Rh(II) centers with a Rh−Rh bond accounting for the diamagnetism. An alternative description of the bonding in **4b** is a diborylmethylammonium complex that would result in the Rh centers being formally Rh(0). The DPEphos ligand adopts a κ^2-PP motif, with two of the phosphines (P2, P3) trans to the BH agostic interaction and cis to the Rh−Rh bond, while P1 and P4 lie trans to the Rh−Rh bond and couple to both Rh centers in the ^{31}P{^{1}H} NMR spectrum [e.g., J(RhP) = 139, 102 Hz]. The four ^{31}P environments are chemically inequivalent. There is no evidence for a Rh−H−Rh bridging hydride (NMR, ESI−MS), and the α-BH···Rh are observed as two broad doublets at δ −8.86 and −9.44 ppm [J(PH) ≈ 70 Hz] in the ^{1}H{^{11}B} NMR spectrum.[34] The ^{11}B NMR spectrum shows a broad signal at δ 9.4 ppm. These data show that the solid-state structure is retained in solution. As the NMeH group forces C_1 symmetry in the molecule, this also shows that the amido−bisboryl ligand is not undergoing rapid and reversible

dissociation or hydride fluxionality. A Quantum Theory of Atoms in Molecules (QTAIM) study of the bonding in the cation of **4b** (Figure 3) indicates a Rh−Rh interaction, with the
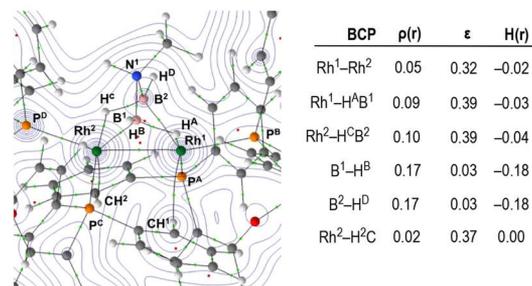

BCP	$\rho(r)$	ε	$H(r)$
Rh^1−Rh^2	0.05	0.32	−0.02
Rh^1−H^{A}B^1	0.09	0.39	−0.03
Rh^2−H^{C}B^2	0.10	0.39	−0.04
B^1−H^B	0.17	0.03	−0.18
B^2−H^D	0.17	0.03	−0.18
Rh^2−H^{2}C	0.02	0.37	0.00

Figure 3. Contour plot of the electron density of the central cationic portion of **4b** presented in the {Rh^{1}N^{1}Rh^2} plane with projected stationary points, bond paths, bond critical points (BCPs; green), and ring critical points (RCPs; red). The associated table shows selected BCP metrics (a.u.; average data for indicated bonds).

presence of a bond path and bond critical point (BCP) between Rh1 and Rh2. BCPs are also present between Rh1− H^{A}B1 and Rh2−H^{C}B2, giving evidence for the α-BH···Rh agostic interactions. This is supported, for example, through examination of the BCP metrics of bridging B1−H^A/B2−H^C, which show a weaker (lower electron density, $\rho(r)$, and total energy density, $H(r)$) B−H bond with less symmetrical bonding (larger ellipticity, ε) than for terminal B1−H^B/B2− H^D, as expected for B−H bonds involved in agostic interactions. Comparatively weak CH···Rh agostic interactions ($\rho(r)$ = 0.02, $H(r)$ = 0.00) between phenyl groups and each Rh center are also observed in the QTAIM analysis and also observed experimentally, e.g., Rh1···C38, 2.997(5) Å. Consistent with such interactions, a broad asymmetric signal is observed at δ 3.94 ppm (2 H) in the ^{1}H NMR spectrum of **4b** that is attributed to agostic Rh···HC$_{phenyl}$ interactions, similar to that observed in [Ru(P^{i}Pr$_3$)$_2$(H)(H$_2$)(C$_6$H$_5$C$_5$H$_4$N)]- [BAr$^F_4$] (δ 4.14 ppm).[35] **4b** is a rare example of a complex with both C−H and B−H agostic interactions.[36,37]

Related structures to **4b** that show bridging "BNB",[20,38] α-BH···Rh agostic,[39] or amino−boryl motifs[9,40] have been reported before. However, as far as we are aware, the amido−bisboryl structure is a new motif in metalloborane chemistry. Perhaps most closely related to **4b** is a Rh-dimer with P−C activated Xantphos-Ph ligands and a bridging N,N-dimethylaminodiboranate unit ([H$_3$BNMe$_2$BH$_3$]$^-$) that is isolated at the end of dehydrocoupling of H$_3$B·NMe$_2$H when using catalyst **A**. Interestingly, this is also a competent catalyst for H$_3$B·NMeH$_2$ dehydropolymerization.[20] While we currently can only speculate on the mechanism of formation of **4**, it is connected to **3** by simple addition of BH$_3$ and loss of H$_2$. Under catalytic conditions **3** likely forms first, while the role of **4** is less clear. To help resolve the identity of the active species in catalysis, kinetic studies were undertaken, taking **2a**, **3a**, and **4b** as precatalysts.

2.4. Kinetic Studies of Dehydropolymerization As Followed by H$_2$ Evolution. The kinetics of dehydropolymerization were followed by volumetric studies of H$_2$ generation using a eudiometer. In all cases ∼1.1 equiv of H$_2$ was measured and very little N-trimethylborazine was observed by ^{11}B NMR spectroscopy (<5%, Figure S23), indicating that evolved H$_2$ is a good proxy for transient[41] H$_2$B=NMeH equivalents formed
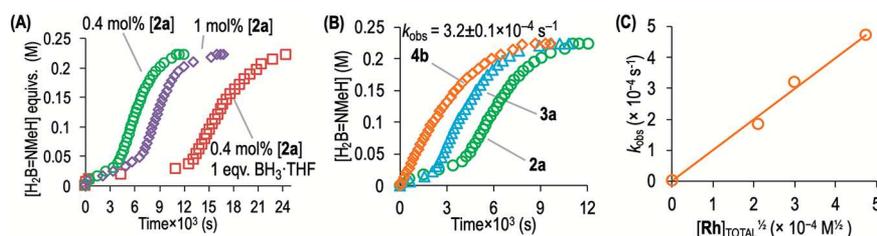
Figure 4. H_2B═$NMeH$ equivalents from H_2 evolution (eudiometer) in the dehydropolymerization of $H_3B \cdot NMeH_2$ (0.223 M 1,2-$F_2C_6H_4$, 20 °C). Each set of comparative runs used the same batch of solvent and $H_3B \cdot NMeH_2$. (A) [**2a**] = 0.4 and 1 mol % Rh and 0.4 mol % + 1 equiv of $H_3B \cdot$ THF; (B) **2a**, **3a**, and **4b** at 0.4 mol % [Rh]$_{TOTAL}$, k_{obs} measured for [**4b**]. (C) [Rh]$_{TOTAL}$ versus k_{obs} using **4b** as a catalyst.

and subsequent polymer chain growth. A significant induction period was observed prior to faster turnover (e.g., ~60 min, 0.4 mol %), that gets *longer* with increase in [**2a**]$_0$ (Figures 4A and S24; e.g., 0.1 mol %, t_{ind} = 33 min; 1 mol %, t_{ind} = 110 min). An induction period has also been noted for catalyst **A** in $H_3B \cdot$ $NMeH_2$ dehydropolymerization[9] as well as for [Rh(Ph$_2$P-(CH$_2$)$_3$PPh$_2$)(FC$_6$H$_5$)][BAr$^F_4$], **C**, in $H_3B \cdot NMe_2H$ dehydro-coupling (10 and 5 min, respectively, at 0.2 mol %).[42] For this latter system, increased [Rh]$_{TOTAL}$ also led to longer induction periods, and a subsequent study showed the initial formation of an amino−borane-bridged dimer analogous to **3a**.[30] While the observation of an induction period might suggest a heterogeneous system here,[43−45] addition of excess Hg or substoichiometric PPh$_3$ during productive turnover did not significantly reduce reaction rate, and no darkening of the reaction was noted, pointing toward homogeneous catalysis (Figure S25). Overall, the kinetics evolve in a sinusoidal manner, with a rate maximum reached approximately at the midpoint (e.g., 0.4 mol %, ν_{max} = 4.1(2) × 10^{-5} M s^{-1}). This behavior is suggestive of a long induction period coupled to rate-attenuation as the substrate is depleted. There is a noninteger dependence of the maximum rate on the initial catalyst concentration (Figure S28), which hints at more complex kinetics. Using 0.223 M $D_3B \cdot NMeH_2$ or $H_3B \cdot NMeD_2$ at 0.4 mol % **2a**, kinetic isotope effects (KIEs) determined from ν_{max} were $k(BH)/k(BD)$ = 1.1 ± 0.1 and $k(NH)/k(ND)$ = 2.2 ± 0.1, which suggests that N−H bond cleavage is involved in the turnover-limiting step. These data are very similar to those measured for **A**.[9] The polymerization is not living as recharging **2a** gives approximately the same M_n, at a similar rate for second recharge (Figure S31). A short induction period was noted for each recharge, which reflects the reformation of **3a** at the end of catalysis (vide infra).

Use of in situ generated dimeric **3a** leads to a shorter, but still significant, induction period (~30 min, Figure 4B) and a similar profile and rate maximum as for **2a**. In contrast, reaction of crude **4b** resulted in no detectable induction period. Furthermore, H_2 evolution (a proxy for H_2B═$NMeH$ formation) followed a first-order profile (Figure 4B, k_{obs} = 3.2(1) × 10^{-4} s^{-1}), and this allowed for a half-order dependency on initial catalyst concentration, i.e., [Rh]$_{TOTAL}$, to be estimated (Figures 4C and S30).

The polymers isolated from these H_2 evolution studies using **3a** and **4b** are similar by GPC analysis but slightly longer compared to that from **2a** at equivalent [Rh]$_{TOTAL}$ (Table 1, entries 7, 9, and 10). Speciation studies at 1 mol % **2a** return only **3a** at the end, which suggests that, if formed, **4a** must be consumed under the conditions of catalysis. Overall these data show the following: a change in H_2-evolution kinetics on moving from **2a** (complex) to **4** (pseudo first-order), that **4**
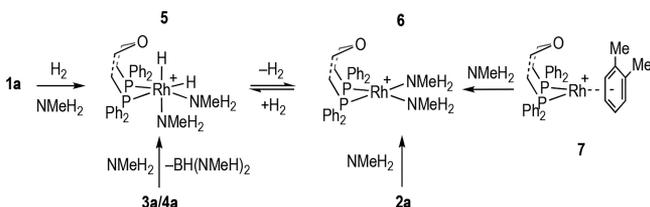
likely sits close to the actual catalyst, and that **3** still requires an induction process to bring it on-cycle. The approximately half-order dependence in [Rh]$_{TOTAL}$ when using **4a** as a precatalyst suggests a lower-order (ligation or nuclearity) active catalyst that is in a rapid equilibrium with a higher-order inactive species, as is discussed later.

2.5. Kinetic Studies: Doping Experiments and the Promoting Effect of NMeH$_2$. Seeking to understand the observed kinetics, and in particular the underlying reason for the induction period, the influence of various species that may be present, or formed, during catalysis was examined. Addition of 1 equiv of $H_3B \cdot$THF (in 50 μL of THF) to 0.4 mol % [**2a**]/$H_3B \cdot NMeH_2$/1,2-$F_2C_6H_4$ solvent increased the induction period significantly (Figure 4A) and gave significantly shorter polymer (Table 1, entry 11), while 10 equiv halts catalysis, possibly by the formation of inactive boron-rich species (see Supporting Information).[32] Added [$H_2B(NMeH_2)_2$][BAr$^F_4$] (10 equiv) significantly slows catalysis, now taking 24 h for completion to produce very short polymer (M_n = 2 800 g/mol, Đ = 2.3). This argues against its role in productive catalysis, in contrast with other systems,[10,29,46] in particular the [Rh-(Xantphos-^{i}Pr)]$^+$ system, where it promotes catalysis.[10] At low relative concentrations, $H_3B \cdot$THF presumably acts to titrate out NMeH$_2$, while we propose that excess [$H_2B(NMeH_2)_2$]$^+$ acts to poison catalysis, possibly sequestering NMeH$_2$ via N−H···NMeH$_2$ hydrogen bonding, as noted for related bis-(phosphine)boronium salts.[47] The control experiment of THF addition (50 μL) reduced the induction period to 30 min and produced polymer comparable to nondoped experiments (Table 1, entry 13). The most dramatic change came from addition of ~2 equiv of NMeH$_2$ (in 50 μL of THF) to 0.4 mol % [**2a**]/$H_3B \cdot NMeH_2$. This resulted in a kinetic profile for H_2 evolution that now showed no induction period and pseudofirst-order kinetics for hydrogen evolution (k_{obs} = 3.7(1) × 10^{-4} s^{-1}), similar to that of **4b** at the same [Rh]$_{TOTAL}$. Isolated polymer, however, was considerably longer (M_n = 27 400 g/mol, Đ = 1.9) than for when just **2a** was used. As expected, under open conditions M_n increases (M_n = 32 100 g/mol, Đ = 1.6), albeit to a lesser extent than compared with the analogous nondoped experiments (cf. entries 14/15 and 2/7, Table 1). These observations, alongside the speciation data at 10 mol %, which demonstrate that **3a** is likely the first formed species, show that free NMeH$_2$ formed from B−N bond cleavage is key to not only bringing the catalyst on-cycle but also promoting propagation or attenuating chain-transfer/termination, leading to higher molecular weights of isolated polymer. Given these observations, the role of NMeH$_2$ was next investigated.

2.6. Rh−Amine Adducts As Effective Precatalysts. We first sought to understand the likely species generated in situ by

addition of amine to the precatalyst, **2a**. Addition of ~2 equiv of NMeH$_2$ (in THF) to **2a** gave the simple bisamine complex [Rh(κ^2-P,P-DPEphos)(NMeH$_2$)$_2$][BAr$^F_4$], **6**, which reacts rapidly (on time of mixing) with H$_2$ in situ to form the corresponding dihydride [Rh(κ^2-P,P-DPEphos)-(H)$_2$(NMeH$_2$)$_2$][BAr$^F_4$], **5** (Scheme 4). Complex **5** reversibly,

Scheme 4. Synthesis of Amine Adducts; [BAr$^F_4$]$^-$ Anions Not Shown and DPEphos Ligand Shown in Truncated Form

Figure 5. (A) H$_2$B═NMeH equivalents from H$_2$ evolution (eudiometer) in the dehydropolymerization of H$_3$B·NMeH$_2$ (0.223 M 1,2-F$_2$C$_6$H$_4$, 20 °C). Each set of comparative runs used the same batch of solvent and H$_3$B·NMeH$_2$. **5/6** (~50:50) at various loadings + 0.05 μL of THF, inset = k_{obs} versus [**5/6**]$^{0.5}$. (B) Comparison of M_n and Đ versus [**5/6**], pure **6**, **2a**, **3a**, and **4b** (under H$_2$-evolution measurement conditions).

but slowly, loses H$_2$ under extended degassing to reform complex **6**, and thus we suggest that, under the conditions of dehydropolymerization, **5** would be persistent. NMR spectroscopic data are fully consistent with the proposed structures (see later), but under these conditions of synthesis isolating pure samples of **5** and **6** in bulk has proved difficult; and a 1:1 mixture of **5/6** is conveniently prepared from **1a**/~2 × NMeH$_2$/H$_2$/degas and used directly in catalysis (see Supporting Information). Complex **5** is the sole organometallic product on addition of ~2 equiv of NMeH$_2$ to a 1:3 mixture of **3a/4a**, alongside HB(NMeH)$_2$ [δ(^{11}B) 28.6 ppm, J(BH) = 127 Hz], demonstrating the role of NMeH$_2$ in both generating **3**, via boronium formation,[29,30] and bringing dimeric **3** and **4** back to monometallic species. Complex **6** (and **5** on subsequent addition of H$_2$ in solution) can be prepared as a free-flowing pure solid in bulk via an alternative route, from addition of NMeH$_2$ to [Rh(κ^2-P,P-DPEphos)(η^6-o-Me$_2$C$_6$H$_4$)][BAr$^F_4$], **7**,[48] which enables definitive characterization by NMR spectroscopy. However, this involves laborious multiple triturations with cold pentane, and thus, the in situ prepared mixture is more convenient to use. Notable NMR spectroscopic data for **6** are the observation of equivalent NMeH$_2$ groups in the ^{1}H NMR spectrum, while for **5** addition of H$_2$ makes these groups inequivalent and diastereotopic; two Rh–H environments are observed, one of which shows a large trans coupling to ^{31}P [J(HP) = 182 Hz], and inequivalent phosphorus environments are observed in the ^{31}P{^{1}H} NMR spectrum (Supporting Information). Data from H$_2$-evolution kinetics and isolated polymer using isolated **6** fit well with the trends apparent from using the **5/6** in situ mixture (Table 1 and Figure 5).

Using in situ generated **5/6** gave pseudo first-order plots for H$_2$ evolution (e.g., 0.4 mol %, k_{obs} = 4.1(1) × 10^{-4} s^{-1}) with no induction period observed. These were also half-order in [Rh]$_{TOTAL}$ (Figure 5A). Half-order behavior is indicative of either a rapid equilibrium between species of different nuclearity, e.g., monomer–dimer, prior to the turnover-limiting step, in which the higher nuclearity species is inactive but dominant,[49] or the rapid and reversible dissociation of a ligand that reveals a low concentration of an active species.[50] Monomer/dimer equilibria have been proposed in polymerization systems previously,[51−53] and in amine−borane dehydrocoupling specifically.[49,54,55] While addition of 10 equiv of NMeH$_2$ caused no significant change in rate (k_{obs} = 4.2(1) × 10^{-4} s^{-1}), suggesting that NMeH$_2$ dissociation is not
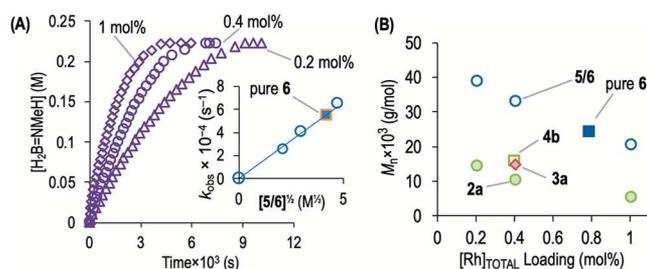
occurring, the polymer isolated from this experiment was insoluble in THF. We thus cannot rule out a change in mechanism. We discount rapid and reversible H$_2$ loss as the reason for the observed half-order kinetics because under conditions of measurement H$_2$ effectively becomes saturated and constant. Speciation studies with excess NMeH$_2$ (10 equiv, [Rh]$_{TOTAL}$ = 5 mol %) revealed **5** to be the only observed organometallic species. No significant change in kinetics was observed on addition of excess Hg, or 0.2 equiv of PPh$_3$, during catalysis—suggesting a homogeneous system.[56] The use of these in situ prepared amine complexes **5/6** leads to polymer with greater M_n (but still inverse with regard to [Rh]$_{TOTAL}$), while Đ is kept relatively low (Figure 5B, e.g., 1 mol %, M_n = 20 600 g/mol, Đ = 1.5). Thus, the added amine—whether bound or free—not only brings the catalyst onto cycle but also promotes greater apparent degrees of polymerization. Whether this is by faster propagation or attenuation of termination is not currently known.

Following catalysis by ^{31}P{^{1}H} NMR spectroscopy using pure **5** (1 mol %) showed that during productive catalysis a single organometallic species is observed (albeit with low signal-to-noise) as a doublet at δ 41 ppm [J(RhP) = 150 Hz], which slowly resolves to complex **3** at the end of catalysis. Importantly, the same species is observed when starting with precatalyst **4b** (0.5 mol %, 1 mol % [Rh]$_{TOTAL}$). This strongly suggests that both precatalysts evolve to a common species—the identity of which remains to be resolved.

Interestingly, the promoting effect of NMeH$_2$ is not operative in the [Rh(Xantphos-^{i}Pr)(H)$_2$]$^+$ system,[10] which is suggested to involve a different mechanism, where dehydrogenation and chain propagation occur at different metal centers in a bifunctional catalyst. Thus, independently prepared [Rh(mer-κ^3-POP-Xantphos-^{i}Pr)(H)$_2$(NMeH$_2$)][BAr$^F_4$], **8** (see Supporting Information), does not dehydropolymerize H$_3$B·NMeH$_2$, returning unchanged substrate after 1 h (0.2 mol %, 0.111 M H$_3$B·NMeH$_2$). This is probably due to the relatively strongly bound amine blocking access of H$_3$B·NMeH$_2$ to the metal center, at which the Xantphos-^{i}Pr is also not hemilabile (Figure S1), so that σ-complex formation by coordination of amine−borane, and subsequent dehydrogenation by BH/NH activation, does not take place. The broader promoting effects of NMeH$_2$ are, however, evident in other cationic {Rh(chelating phosphine)}$^+$ systems that are suggested to undergo a coordination/dehydrogenation/chain-growth mechanism. Under the specific conditions reported here, both [Rh(Xantphos-Ph)]$^+$, **A**,[9] and [Rh(Ph$_2$P-

Table 2. Effect of Added Amine in Selected Cationic Rh Catalysts, M_n (g/mol) and Đ; 0.223 M, 0.2 mol % Catalyst, H_2 Measurement Conditions, 1,2-$F_2C_6H_4$; [BAr^F_4]$^-$ Anions Not Shown

catalyst	no added amine	~2 equiv of $NMeH_2$
[Rh(DPEphos)($H_2B(NMe_3)(CH_2)_2{}^tBu$)]$^+$ **2a**	14500 (1.7)	34800 (1.5)
[Rh(Xantphos-Ph)($H_2B(NMe_3)(CH_2)_2{}^tBu$)]$^+$ **A**	40500 (1.7)	60900 (1.6)
[Rh($PH_2P(CH_2)_3PPh_2$)(C_6H_5F)]$^+$ **C**	63100 (1.7)	78900 (1.6)

$(CH_2)_3PPh_2)]^+$, **C**,[16,42] systems show increased M_n, slightly lower Đ, and no induction periods when ~2 equiv of $NMeH_2$ is added to the precatalyst, compared to the nondoped controls (Table 2).

**2.7. Discussion of Proposed Mechanistic Landscape.** Bringing these observations together, we propose an overall mechanism shown in Scheme 5, in which the induction period

Scheme 5. Pathways for Catalyst Activation and Catalysis in the Dehydropolymerization of $H_3B\cdot NMeH_2$ Using [Rh] = {Rh(DPEphos)}$^+$ Precatalysts[a]
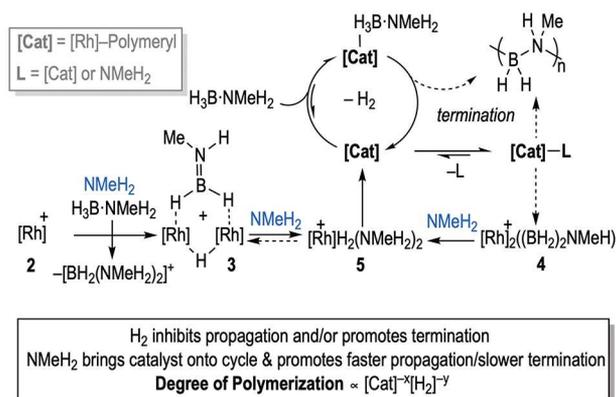
^{a}Anions are not shown. [Cat] may be mono- or bimetallic.

that gets longer with increased [**2a**] can also now be explained. $NMeH_2$, generated by slow B−N bond cleavage of $H_3B\cdot NMeH_2$, at a rate that is independent of [**2a**], first promotes the formation of **3a** and then more slowly the active precatalyst **5**. In this model, higher concentrations of **2a** result in more **3a** needing to be first formed, via hydride abstraction and boronium formation, and then converted to the active catalyst with an unchanged amount of $NMeH_2$, thus leading to a longer induction period. The active catalyst is closely related to both **5/6** and **4a**, but we suggest both of these sit outside of the productive cycle, as their structures and reactivity are incompatible with the observed kinetics. The insensitivity in rate to added $NMeH_2$ *suggests* this does not reversibly dissociate, while a sensible model in which dimeric **4a**, with its Rh−Rh bond and bridging amido−bisboryl ligand, undergoes rapid and reversible dissociation (vide supra) or loss of ligand is not obvious. Moreover, **4b** reacts rapidly with $NMeH_2$ to form **5**, suggesting that if formed in catalysis it is not persistent. In addition, the fact that both **5** and **4b** evolved to the same, currently unresolved, organometallic species under catalytic conditions suggests that both sit just outside of the productive catalytic cycle. While we cannot currently confidently comment on the nature of the actual catalyst for dehydrogenation, chain growth, or the termination process, the half-order relationship in [Rh]$_{TOTAL}$ and the observation of dimeric species (**3** and **4**) suggest that such Rh_2 motifs may be intimately involved. The strong, and persistent, inverse

relationship between M_n and [Rh]$_{TOTAL}$, coupled with the sensitivity to H_2, suggests a coordination/insertion/chain-growth mechanism for which $NMeH_2$ also modifies chain length—possibly by attenuating chain termination. On the basis of the half-order kinetics observed from the dehydrogenation studies, we suggest three possible general motifs for the active catalyst (Scheme 6): one which invokes a monomer−

Scheme 6. Generalized Possible Active Species in Catalysis[a]
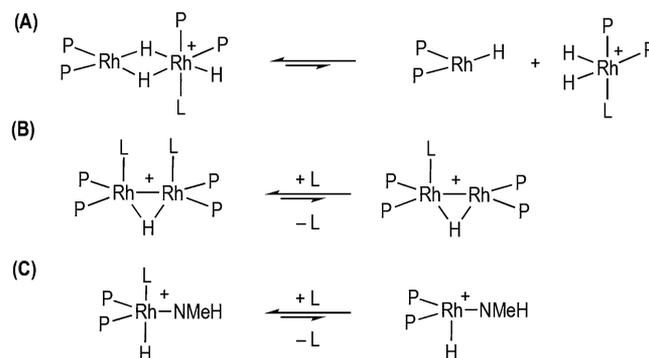
^{a}P = phosphine, L = ligand (e.g., $NMeH_2$, or amine−borane-derived fragment). All structures shown are representative, and the actual number of hydrides/coordination geometry is undetermined.

dimer equilibrium in which one of the monomers is the active catalyst (A), and one in which a persistent dimer reversibly loses a bound ligand (B). Scenario A is reminiscent of the unsymmetrical Rh_2 hydride dimers that can form in Rh-catalyzed alkene hydrogenations,[57] while scenario B is supported by the recent report that dimeric early transition-metal complexes have been shown to act as competent catalysts for $H_3B\cdot NMeH_2$ dehydropolymerization.[7] A third possibility is that deprotonation of bound $NMeH_2$ provides an active Rh−NMeH amido motif, similar to the bifunctional catalysts developed by Schneider and co-workers (C).[11]

3. CONCLUSIONS

We have shown that a combination of catalyst loading, H_2, and $NMeH_2$ can be used to control the dehydropolymerization of $H_3B\cdot NMeH_2$ in a {Rh(DPEphos}$^+$-based catalyst. We proposed this to be an important observation and one that may show some generality, building upon the already demonstrated improvement in catalyst lifetimes on addition of amine.[8] The ability to control polymerization by catalyst loading, $NMeH_2$ addition, and H_2 in {Rh(DPEphos)}$^+$ and {Rh(Xantphos-Ph)}$^+$ systems is markedly different from that found for the {Rh(Xantphos-^{i}Pr)}$^+$ catalyst and further supports that a different mechanism operates between the two sets, which may be related to the preferred coordination geometry of the ligands: DPEphos and Xantphos-Ph prefer *cis*-κ^2-P,P while Xantphos-^{i}Pr generally adopts *mer*-κ^2-P,O,P motifs. The amine systems we describe thus provide a tractable platform for further detailed mechanistic studies, and efforts

are directed to determining the details of the propagating species and termination events so that fine control of the overall process, and thus the polymer produced, can be realized. It will be interesting to see if this effect of added amine is a more general observation across the now numerous[2,3] dehydropolymerization catalysts from across the transition metals.

■ ASSOCIATED CONTENT

Ⓢ Supporting Information

The Supporting Information is available free of charge on the ACS Publications website at DOI: 10.1021/acscatal.9b00081.

> Full experimental section, characterization details, kinetic data and details of the DFT calculated structure, and QTAIM analysis of **4b** (PDF)
>
> Crystallographic data (CIF)

■ AUTHOR INFORMATION

Corresponding Author
*E-mail: andrew.weller@chem.ox.ac.uk.

ORCID Ⓘ
David E. Ryan: 0000-0001-8381-9502
Alasdair I. McKay: 0000-0002-6859-172X
Guy C. Lloyd-Jones: 0000-0003-2128-6864
Andrew S. Weller: 0000-0003-1646-8081

Present Address
∥School of Chemistry, University of Manchester, Oxford Road, Manchester M13 9PL, United Kingdom.

Notes
The authors declare no competing financial interest.

■ ACKNOWLEDGMENTS

■ REFERENCES

(1) Leitao, E. M.; Jurca, T.; Manners, I. Catalysis in Service of Main Group Chemistry Offers a Versatile Approach to P-Block Molecules and Materials. *Nat. Chem.* **2013**, *5*, 817−829.

(2) Colebatch, A. L.; Weller, A. S. Amine-Borane Dehydropolymerization: Challenges and Opportunities. *Chem. - Eur. J.* **2019**, *25*, 1379−1390.

(3) Han, D.; Anke, F.; Trose, M.; Beweries, T. Recent Advances in Transition Metal Catalysed Dehydropolymerisation of Amine Boranes and Phosphine Boranes. *Coord. Chem. Rev.* **2019**, *380*, 260−286.

(4) Staubitz, A.; Robertson, A. P. M.; Sloan, M. E.; Manners, I. Amine− and Phosphine−Borane Adducts: New Interest in Old Molecules. *Chem. Rev.* **2010**, *110*, 4023−4078.

(5) Staubitz, A.; Presa Soto, A.; Manners, I. Iridium-Catalyzed Dehydrocoupling of Primary Amine-Borane Adducts: A Route to High Molecular Weight Polyaminoboranes, Boron-Nitrogen Analogues of Polyolefins. *Angew. Chem., Int. Ed.* **2008**, *47*, 6212−6215.

(6) Dietrich, B. L.; Goldberg, K. I.; Heinekey, D. M.; Autrey, T.; Linehan, J. C. Iridium-Catalyzed Dehydrogenation of Substituted Amine Boranes: Kinetics, Thermodynamics, and Implications for Hydrogen Storage. *Inorg. Chem.* **2008**, *47*, 8583−8585.

(7) Trose, M.; Reiß, M.; Reiß, F.; Anke, F.; Spannenberg, A.; Boye, S.; Lederer, A.; Arndt, P.; Beweries, T. Dehydropolymerisation of Methylamine Borane Using a Dinuclear 1,3-Allenediyl Bridged Zirconocene Complex. *Dalton Trans.* **2018**, *47*, 12858−12862.

(8) Glüer, A.; Förster, M.; Celinski, V. R.; Schmedt auf der Günne, J.; Holthausen, M. C.; Schneider, S. A Highly Active Iron Catalyst for Ammonia Borane Dehydrocoupling at Room Temperature. *ACS Catal.* **2015**, *5*, 7214−7217.

(9) Johnson, H. C.; Leitao, E. M.; Whittell, G. R.; Manners, I.; Lloyd-Jones, G. C.; Weller, A. S. Mechanistic Studies of the Dehydrocoupling and Dehydropolymerization of Amine-Boranes Using a [Rh(Xantphos)]⁺ Catalyst. *J. Am. Chem. Soc.* **2014**, *136*, 9078−9093.

(10) Adams, G. M.; Colebatch, A. L.; Skornia, J. T.; McKay, A. I.; Johnson, H. C.; Lloyd-Jones, G. C.; Macgregor, S. A.; Beattie, N. A.; Weller, A. S. Dehydropolymerization of $H_3B\cdot NMeH_2$ to Form Polyaminoboranes Using [Rh(Xantphos-Alkyl)] Catalysts. *J. Am. Chem. Soc.* **2018**, *140*, 1481−1495.

(11) Marziale, A. N.; Friedrich, A.; Klopsch, I.; Drees, M.; Celinski, V. R.; Schmedt auf der Günne, J.; Schneider, S. The Mechanism of Borane−Amine Dehydrocoupling with Bifunctional Ruthenium Catalysts. *J. Am. Chem. Soc.* **2013**, *135*, 13342−13355.

(12) Staubitz, A.; Sloan, M. E.; Robertson, A. P. M.; Friedrich, A.; Schneider, S.; Gates, P. J.; Schmedt auf der Günne, J.; Manners, I. Catalytic Dehydrocoupling/Dehydrogenation of N-Methylamine-Borane and Ammonia-Borane: Synthesis and Characterization of High Molecular Weight Polyaminoboranes. *J. Am. Chem. Soc.* **2010**, *132*, 13332−13345.

(13) Rossin, A.; Peruzzini, M. Ammonia−Borane and Amine−Borane Dehydrogenation Mediated by Complex Metal Hydrides. *Chem. Rev.* **2016**, *116*, 8848−8872.

(14) De Albuquerque Pinheiro, C. A.; Roiland, C.; Jehan, P.; Alcaraz, G. Solventless and Metal-Free Synthesis of High-Molecular-Mass Polyaminoboranes from Diisopropylaminoborane and Primary Amines. *Angew. Chem., Int. Ed.* **2018**, *57*, 1519−1522.

(15) Jurca, T.; Dellermann, T.; Stubbs, N. E.; Resendiz-Lara, D. A.; Whittell, G. R.; Manners, I. Step-Growth Titanium-Catalysed Dehydropolymerisation of Amine−Boranes. *Chem. Sci.* **2018**, *9*, 3360−3366.

(16) Colebatch, A. L.; Hawkey Gilder, B. W.; Whittell, G. R.; Oldroyd, N. L.; Manners, I.; Weller, A. S. A General, Rhodium-Catalyzed, Synthesis of Deuterated Boranes and N-Methyl Polyaminoboranes. *Chem. - Eur. J.* **2018**, *24*, 5450−5455.

(17) Jenkins, A. D.; Jones, R. G.; Moad, G. Terminology for Reversible-Deactivation Radical Polymerization Previously Called "Controlled" Radical or "Living" Radical Polymerization. *Pure Appl. Chem.* **2009**, *82*, 483−491.

(18) Kranenburg, M.; van der Burgt, Y. E. M.; Kamer, P. C. J.; van Leeuwen, P. W. N. M.; Goubitz, K.; Fraanje, J. New Diphosphine Ligands Based on Heterocyclic Aromatics Inducing Very High Regioselectivity in Rhodium-Catalyzed Hydroformylation: Effect of the Bite Angle. *Organometallics* **1995**, *14*, 3081−3089.

(19) Esteruelas, M. A.; Nolis, P.; Oliván, M.; Oñate, E.; Vallribera, A.; Vélez, A. Ammonia Borane Dehydrogenation Promoted by a Pincer-Square-Planar Rhodium(I) Monohydride: A Stepwise Hydrogen Transfer from the Substrate to the Catalyst. *Inorg. Chem.* **2016**, *55*, 7176−7181.

(20) Johnson, H. C.; Weller, A. S. P−C-Activated Bimetallic Rhodium Xantphos Complexes: Formation and Catalytic Dehydrocoupling of Amine−Boranes. *Angew. Chem., Int. Ed.* **2015**, *54*, 10173−10177.

(21) Adams, G. M.; Weller, A. S. POP-Type Ligands: Variable Coordination and Hemilabile Behaviour. *Coord. Chem. Rev.* **2018**, *355*, 150−172.

(22) Johnson, H. C.; McMullin, C. L.; Pike, S. D.; Macgregor, S. A.; Weller, A. S. Dehydrogenative Boron Homocoupling of an Amine−Borane. *Angew. Chem., Int. Ed.* **2013**, *52*, 9776−9780.

(23) Merle, N.; Koicok-Köhn, G.; Mahon, M. F.; Frost, C. G.; Ruggerio, G. D.; Weller, A. S.; Willis, M. C. Transition Metal Complexes of the Chelating Phosphine Borane Ligand $Ph_2PCH_2PH_2P\cdot BH_3$. *Dalton Trans.* **2004**, 3883−3892.

(24) Johnson, H. C.; Torry-Harris, R.; Ortega, L.; Theron, R.; McIndoe, J. S.; Weller, A. S. Exploring the Mechanism of the Hydroboration of Alkenes by Amine−Boranes Catalysed by [Rh-(Xantphos)]⁺. *Catal. Sci. Technol.* **2014**, *4*, 3486−3494.

(25) Han, D.; Joksch, M.; Klahn, M.; Spannenberg, A.; Drexler, H. J.; Baumann, W.; Jiao, H.; Knitsch, R.; Hansen, M. R.; Eckert, H.; Beweries, T. Iridium(III) Hydrido Complexes for the Catalytic Dehydrogenation of Hydrazine Borane. *Dalton Trans.* **2016**, *45*, 17697−17704.

(26) Kim, J.; Soares, J.; Rempel, G. Use of Hydrogen for the Tailoring of the Molecular Weight Distribution of Polyethylene in a Bimetallic Supported Metallocene Catalyst System. *Macromol. Rapid Commun.* **1998**, *19*, 197−199.

(27) Ravve, A. *Principles of Polymer Chemistry*, 3rd ed.; Springer: New York, 2012.

(28) Johnson, H. C.; Robertson, A. P. M.; Chaplin, A. B.; Sewell, L. J.; Thompson, A. L.; Haddow, M. F.; Manners, I.; Weller, A. S. Catching the First Oligomerization Event in the Catalytic Formation of Polyaminoboranes: H₃B·NMeHBH₂·NMeH₂ bound to Iridium. *J. Am. Chem. Soc.* **2011**, *133*, 11076−11079.

(29) Roselló-Merino, M.; López-Serrano, J.; Conejero, S. Dehydrocoupling Reactions of Dimethylamine-Borane by Pt(II) Complexes: A New Mechanism Involving Deprotonation of Boronium Cations. *J. Am. Chem. Soc.* **2013**, *135*, 10910−10913.

(30) Kumar, A.; Beattie, N. A.; Pike, S. D.; Macgregor, S. A.; Weller, A. S. The Simplest Amino−Borane H₂B=NH₂ Trapped on a Rhodium Dimer: Pre-Catalysts for Amine−Borane Dehydropolymerization. *Angew. Chem., Int. Ed.* **2016**, *55*, 6651−6656.

(31) Colebatch, A. L.; McKay, A. I.; Beattie, N. A.; Macgregor, S. A.; Weller, A. S. Fluoroarene Complexes with Small Bite Angle Bisphosphines: Routes to Amine−Borane and Aminoborylene Complexes: Fluoroarene Complexes with Small Bite Angle Bisphosphines: Routes to Amine−Borane and Aminoborylene Complexes. *Eur. J. Inorg. Chem.* **2017**, *2017*, 4533−4540.

(32) B−N bond cleavage would also generate "BH₃". At 10 mol % **2a**/H₃B·NMeH₂, ESI−MS shows the formation of **3a**, **4a**, and an additional species with the empirical formula [Rh₂(DPEphos)₂(B₂H₅)]⁺, *m/z* = 1309.16. Addition of H₃B·THF to **2a** gives this as the dominant species. Bridging B₂H₅ units have been previously reported, e.g.: Jacobsen, G. B.; Andersen, E.; Housecroft, C. E.; Hong, F. E.; Buhl, M. L.; Long, G. J.; Fehlner, T. P. Main-Group Chemistry in a Metal Framework: Preparation and Characterization of (Diborane)hexacarbonyldiiron and its Conjugate Base [B₂H5Fe₂(CO)₆]. *Inorg. Chem.* **1987**, *26*, 4040−4046.

(33) Riddlestone, I. M.; Kraft, A.; Schaefer, J.; Krossing, I. Taming the Cationic Beast: Novel Developments in the Synthesis and Application of Weakly Coordinating Anions. *Angew. Chem., Int. Ed.* **2018**, *57*, 13982−14024.

(34) For {Rh(Xantphos-Ph)}⁺ a similar signal was observed at 5 mol %/H₃B·NMe₂H. We speculated upon a *β*-BH−agostic−amidoborane motif, but an alternative formulation could be a structure similar to **4**.

(35) Toner, A.; Matthes, J.; Gründemann, S.; Limbach, H.-H.; Chaudret, B.; Clot, E.; Sabo-Etienne, S. Agostic Interaction and Intramolecular Proton Transfer from the Protonation of Dihydrogen Ortho Metalated Ruthenium Complexes. *Proc. Natl. Acad. Sci. U. S. A.* **2007**, *104*, 6945.

(36) Cassen, A.; Gloaguen, Y.; Vendier, L.; Duhayon, C.; Poblador-Bahamonde, A.; Raynaud, C.; Clot, E.; Alcaraz, G.; Sabo-Etienne, S. B−H, C−H, and B−C Bond Activation: The Role of Two Adjacent Agostic Interactions. *Angew. Chem., Int. Ed.* **2014**, *53*, 7569−7573.

(37) Rudolf, G. C.; Hamilton, A.; Orpen, A. G.; Owen, G. R. A 'Sting' on Grubbs' Catalyst: An Insight into Hydride Migration between Boron and a Transition Metal. *Chem. Commun.* **2009**, 553−555.

(38) Daly, S. R.; Kim, D. Y.; Girolami, G. S. Lanthanide N,N-Dimethylaminodiboranates as a New Class of Highly Volatile Chemical Vapor Deposition Precursors. *Inorg. Chem.* **2012**, *51*, 7050−7065.

(39) Chaplin, A. B.; Weller, A. S. B−H Activation at a Rhodium(I) Center: Isolation of a Bimetallic Complex Relevant to the Transition-Metal-Catalyzed Dehydrocoupling of Amine−Boranes. *Angew. Chem., Int. Ed.* **2010**, *49*, 581−584.

(40) Tang, C. Y.; Phillips, N.; Bates, J. I.; Thompson, A. L.; Gutmann, M. J.; Aldridge, S. Dimethylamine Borane Dehydrogenation Chemistry: Syntheses, X-Ray and Neutron Diffraction Studies of 18-Electron Aminoborane and 14-Electron Aminoboryl Complexes. *Chem. Commun.* **2012**, *48*, 8096−8098.

(41) Metters, O. J.; Chapman, A. M.; Robertson, A. P. M.; Woodall, C. H.; Gates, P. J.; Wass, D. F.; Manners, I. Generation of Aminoborane Monomers RR'N=BH₂ from Amine−Boronium Cations [RR'NHBH₂L]⁺: Metal Catalyst-Free Formation of Polyaminoboranes at Ambient Temperature. *Chem. Commun.* **2014**, *50*, 12146−12149.

(42) Dallanegra, R.; Robertson, A. P. M.; Chaplin, A. B.; Manners, I.; Weller, A. S. Tuning the [L₂Rh···H₃B·NR₃]⁺ Interaction Using Phosphine Bite Angle. Demonstration by the Catalytic Formation of Polyaminoboranes. *Chem. Commun.* **2011**, *47*, 3763−3765.

(43) Crooks, A. B.; Yih, K.-H.; Li, L.; Yang, J. C.; Özkar, S.; Finke, R. G. Unintuitive Inverse Dependence of the Apparent Turnover Frequency on Precatalyst Concentration: A Quantitative Explanation in the Case of Ziegler-Type Nanoparticle Catalysts Made from [(1,5-COD)Ir(μ-O₂C₈H₁₅)]₂ and AlEt₃. *ACS Catal.* **2015**, *5*, 3342−3353.

(44) Jaska, C. A.; Manners, I. Heterogeneous or Homogeneous Catalysis? Mechanistic Studies of the Rhodium-Catalyzed Dehydrocoupling of Amine−Borane and Phosphine−Borane Adducts. *J. Am. Chem. Soc.* **2004**, *126*, 9776−9785.

(45) Sonnenberg, J. F.; Morris, R. H. Distinguishing Homogeneous from Nanoparticle Asymmetric Iron Catalysis. *Catal. Sci. Technol.* **2014**, *4*, 3426−3438.

(46) Pal, S.; Kusumoto, S.; Nozaki, K. Dehydrogenation of Dimethylamine−Borane Catalyzed by Half-Sandwich Ir and Rh Complexes: Mechanism and the Role of Cp* Noninnocence. *Organometallics* **2018**, *37*, 906−914.

(47) Shuttleworth, T. A.; Huertos, M. A.; Pernik, I.; Young, R. D.; Weller, A. S. Bis(Phosphine)Boronium Salts. Synthesis, Structures and Coordination Chemistry. *Dalton Trans.* **2013**, *42*, 12917−12925.

(48) Hooper, J. F.; Chaplin, A. B.; González-Rodríguez, C.; Thompson, A. L.; Weller, A. S.; Willis, M. C. Aryl Methyl Sulfides as Substrates for Rhodium-Catalyzed Alkyne Carbothiolation: Arene Functionalization with Activating Group Recycling. *J. Am. Chem. Soc.* **2012**, *134*, 2906−2909.

(49) Sewell, L. J.; Huertos, M. A.; Dickinson, M. E.; Weller, A. S.; Lloyd-Jones, G. C. Dehydrocoupling of Dimethylamine Borane Catalyzed by Rh(PCy₃)₂H₂Cl. *Inorg. Chem.* **2013**, *52*, 4509−4516.

(50) Boller, T. M.; Murphy, J. M.; Hapke, M.; Ishiyama, T.; Miyaura, N.; Hartwig, J. F. Mechanism of the Mild Functionalization of Arenes by Diboron Reagents Catalyzed by Iridium Complexes. Intermediacy and Chemistry of Bipyridine-Ligated Iridium Trisboryl Complexes. *J. Am. Chem. Soc.* **2005**, *127*, 14263−14278.

(51) Shapiro, P. J.; Schaefer, W. P.; Labinger, J. A.; Bercaw, J. E.; Cotter, W. D. Model Ziegler-Natta Α-Olefin Polymerization Catalysts Derived from [{(η⁵-C₅Me₄)SiMe₂(η¹-NCMe₃)}(PMe₃)Sc(η²-H)]₂ and [{(η⁵-C₅Me₄)SiMe₂(η¹-NCMe₃)}Sc(η²-CH₂CH₂CH₃)]₂. Synthesis, Structures, and Kinetic and Equilibrium Investigations of the Catalytically Active Species in Solution. *J. Am. Chem. Soc.* **1994**, *116*, 4623−4640.

(52) Chamberlain, B. M.; Jazdzewski, B. A.; Pink, M.; Hillmyer, M. A.; Tolman, W. B. Controlled Polymerization of Dl-Lactide and Ε-Caprolactone by Structurally Well-Defined Alkoxo-Bridged Di- and Triyttrium(III) Complexes. *Macromolecules* **2000**, *33*, 3970−3977.

(53) Bochmann, M.; Lancaster, S. J. Monomer−Dimer Equilibria in Homo- and Heterodinuclear Cationic Alkylzirconium Complexes and Their Role in Polymerization Catalysis. *Angew. Chem., Int. Ed.* **1994**, *33*, 1634−1637.

(54) Kumar, A.; Ishibashi, J. S. A.; Hooper, T. N.; Mikulas, T. C.; Dixon, D. A.; Liu, S.-Y.; Weller, A. S. The Synthesis, Characterization

and Dehydrogenation of Sigma-Complexes of BN-Cyclohexanes. *Chem. - Eur. J.* **2016**, *22*, 310−322.

(55) Zhang, X.; Kam, L.; Trerise, R.; Williams, T. J. Ruthenium-Catalyzed Ammonia Borane Dehydrogenation: Mechanism and Utility. *Acc. Chem. Res.* **2017**, *50*, 86−95.

(56) Widegren, J. A.; Finke, R. G. A Review of the Problem of Distinguishing True Homogeneous Catalysis from Soluble or Other Metal-Particle Heterogeneous Catalysis under Reducing Conditions. *J. Mol. Catal. A: Chem.* **2003**, *198*, 317−341.

(57) Duckett, S. B.; Newell, C. L.; Eisenberg, R. Observation of New Intermediates in Hydrogenation Catalyzed by Wilkinson's Catalyst, RhCl(PPh$_3$)$_3$, Using Parahydrogen-Induced Polarization. *J. Am. Chem. Soc.* **1994**, *116*, 10548−10556.